Magnetotransport properties of lateral-surface superlattices by molecular-dynamics Monte Carlo simulation

Toshishige Yamada and D. K. Ferry

Center for Solid State Electronics Research, Arizona State University, Tempe, Arizona 85287-6206

The magnetotransport properties of a lateral-surface superlattice, a two-dimensional (2D) electron system in a 2D periodic potential, are studied with use of a Monte Carlo technique, where the effect of the magnetic field is included through a Lorentz force and the interparticle Coulomb interaction is included with a molecular-dynamics method. Excellent numerical energy conservation is achieved by adopting a predictor-corrector algorithm to integrate the equations of motion. The simulation shows that the diffusion constant, as a function of the magnetic field, is not a simple monotone function but has a structure with multiple minima. This structure is attributed to the correlated circular electron motion, and this is reminiscent of classical pinning orbits in a 2D antidot array, even in the presence of the Coulomb interaction. The radial-distribution function shows no significant dependence upon the magnetic field up to ten flux quanta per unit cell.

I. INTRODUCTION

A two-dimensional (2D) electron gas in a 2D periodic potential with the period $a \sim 0.1$ μm can now experimentally be achieved in lateral-surface superlattices (LSSL's) embedded in field-effect transistor (FET) structures with a mesh-gate electrode.[1−3] In these systems, the magnetic length $(\hbar/eB)^{1/2}$ for one flux quanta per unit cell is ~ 0.04 μm $(\Phi/\Phi_0 = a^2/2\pi l_B^2)$. The 2D potential can often be represented by a smooth function, which is the summation of the two cosine functions, $V(x,y) = V_0/4$ $[\cos(2\pi x/a) + \cos(2\pi y/a) + 2]$ with peak-to-peak amplitude V_0. If the characteristic electron energy E is smaller than the saddle-point energy $V_0/2$, electrons are mainly confined in the 2D potential minima and an array of quantum dots is formed. If $V_0/2 < E < V_0$, electrons basically move freely except for those regions where the 2D potential energy is larger than E and an array of antidots is formed. Recently, the magnetotransport properties of 2D electrons, in the latter case of a 2D antidot array, have been studied experimentally,[4] and the magnetoresistance shows peaks when the cyclotron radius can enclose a fixed number of antidots ($n = 1,2,4,9,21$ in the experiment). This "pinning" of the cyclotron orbit is explained by a classical pinball model.[4] Resistance minima occur when the cyclotron orbit is not commensurate with the lattice period, resulting in diffusive transport where the orbit is specularly reflected by the antidot potential.

The key assumption for the pinball model is that the number of electrons in a unit cell is so large that the interparticle Coulomb interaction is well screened, and as a result, a noninteracting, independent electron picture prevails with the Fermi energy as the characteristic electron energy. If we reduce the number of electrons in a unit cell, the screening becomes weaker and all electrons are bound to one another through the Coulomb interaction. The motion of a particular electron affects that of other electrons and there is nonlinear feedback to the

original electron. In thermal equilibrium without the Coulomb interaction when $V_0 \gg k_B T$, electrons prefer to stay near the bottom of the 2D potential well. The typical separation of electrons for a potential depth $\sim 10 k_B T$ would be $d \sim a/10 \sim 0.01$ μm.[5] This small separation causes an unscreened interparticle Coulomb energy $1/(4\pi\epsilon d)$ as large as ~ 11 meV (in a GaAs channel). At 4.2 K, this value is much larger than the thermal energy and electrons are driven apart some reasonable distance, which increases the average potential energy of these electrons. Under this situation, the Coulomb interaction is expected to have a significant effect on the dynamics of the carriers.

In order to clarify this, we have studied the effect of the Coulomb interaction on the magnetotransport properties with a Monte Carlo model incorporating a molecular-dynamics technique,[5] the latter of which is a straightforward method to include the Coulomb interaction.[6] At each time step, the Coulomb force is calculated for all pairs of electrons and their positions and momenta are updated according to this force. The advantage of this method is that it makes no assumption about screening or collective mode excitations. These effects are automatically included in molecular dynamics. In order to eliminate unwanted effects from the use of the finite number of electrons in simulations, periodic boundary conditions are adopted and the Coulomb force is calculated with a method based on the Ewald sum. These treatments enable us to simulate virtually an infinitely large system. The effect of the magnetic field is included through a Lorentz force. Thermal equilibrium is assumed in all the simulations here and the diffusion constant is evaluated by the temporal derivative of an Einstein plot, i.e., the plot of the mean-square displacement of electrons versus time. Scattering by both impurity (with a concentration of $N_I = 3.3 \times 10^{15}$ cm^{-3}, uniformly distributed through the Ga$_{1-x}$Al$_x$As layer of the heterostructure) and by phonons is included in the simulation

with a usual Monte Carlo technique, using an envelope function[7] for the lowest subband in the heterojunction inversion layer channel to calculate the scattering rates. Phonon scattering is infrequent on the time scale of interest at this low temperature, and the number of electrons is fixed. Thus, the total electron energy, which is the summation of the particle's kinetic energy, their potential energy, and the interparticle Coulomb energy, has to be conserved (even with phonon emission/absorption, the energy conservation can be extended to include the phonon energy transfer). In this situation, achieving good numerical energy conservation is necessary. We have used an algorithm, stable to second order, based upon a predictor-corrector method to integrate the equations of motion, with double precision used in the code to minimize round-off error, and succeeded in achieving energy conservation, to five significant digit numerical accuracy, during typical simulation runs.

The simulation results show that the diffusion constant does not decrease monotonically with the magnetic field, but has a structure with several minima. This structure is attributed to the correlated circular electron motion, and is reminiscent of the classical pinning orbits in the 2D antidot array, even at low density and in the presence of the Coulomb interaction. This indicates that the pinball model has a much wider applicability than expected originally, and can explain magnetoconductance oscillations that are experimentally observed.

In Sec. II, the model and the numerical techniques are explained, and in Sec. III, the results and discussion are given. This system, a 2D electron gas subject to both a 2D periodic potential and a magnetic field, also has been attracting considerable attention for decades because of the quantum-mechanical energy-band structure, often called a "Hofstadter butterfly," which is a fractal energy band structure with the period of either the number of flux quanta per unit cell or the number of unit cell per flux quanta.[8] This formal aspect of the system has motivated an extensive study of transport properties, and the magnetoresistance shows periodicity either with respect to the magnetic field[1] or with the inverse of the magnetic field.[2,9] The present semiclassical approach cannot predict these quantum structure effects, but we do discuss some of the quantum connections in the Appendix.

II. SIMULATION METHOD

The electrons are considered as classical particles, rather than quantum-mechanical wave packets, moving in a 2D potential, created in a gated GaAs structure, $V(x,y)=V_0/4[\cos(2\pi x/a)+\cos(2\pi y/a)+2]$ with $a=0.16$ μm. (The dimensions were chosen to agree with the experiments of Ref. 1.) The electron area density is taken to be 1.4×10^{10} cm^{-2}, for which the Fermi wave vector and the Fermi energy are 3.0×10^5 cm^{-1} and 0.39 meV, respectively, with a parabolic-band assumption. Since the Fermi energy is on the order of the thermal energy, 0.36 meV (at 4.2 K), degeneracy is not an important effect and we use a classical particle picture.[10] On the other hand, because of the low areal density, the screen-

ing is weak and the Coulomb interaction is essential in the present case,[11] as was discussed in the preceding section. The effects of the Coulomb interaction and the magnetic field are included directly in the electron dynamics and the energy band is assumed to remain parabolic.

We have chosen the 2D potential amplitude $V_0=2.5$ meV since the electrons have previously been found to be in a mobile phase,[5] and the average electron energy lies between the saddle-point energy $V_0/2$ and the maximum barrier height V_0. This situation also is comparable to that of the antidot experiments.[4] Realistic impurity and phonon scattering are included in the ensemble Monte Carlo method as discrete events, although impurity scattering dominates at this low temperature. The strength of the impurity scattering is such that the mobility is 1.3×10^5 cm^2/V s. Electrons perform a free flight under the influence of a Lorentz force caused by the interparticle potential, the 2D potential,[12] and the magnetic field. If scattering occurs, the electrons suddenly change their momentum (and energy in inelastic processes) and then start another free flight. The scattering is a stochastic process and whether or not it occurs is determined in the Monte Carlo code with the usual help of random numbers. We have adopted an envelope function corresponding to the lowest subband in the FET channel after Fang, Howard, and Stern[7] to evaluate the scattering rates in the quasi-two-dimensional inversion channel.

The interparticle Coulomb interaction is treated through a molecular-dynamics technique.[6] At each time step, the Coulomb force is calculated for all electrons and this is used to update the position and momentum of each electron during the subsequent time step through the Lorentz force. In this way, we include various many-body effects automatically without using any artificial assumptions for the screening or the collective excitation mode. In order to eliminate unwanted boundary effects due to the finite number of electrons used, a periodic boundary condition is employed, which enables us to simulate virtually an infinitely large system.[5] We simulate 32 electrons in 3×3 unit cells, corresponding to the electron areal density 1.4×10^{10} cm^{-2}, and the periodic boundary condition is imposed for this simulation square with side length $L=3a$. When an electron leaves the square by crossing the boundary $x=L$, another electron is input from the equivalent boundary $x=0$ with the same y coordinate and the same momentum and energy. The number of electrons in the square remains constant throughout the simulation.

The Coulomb interaction has to be consistently defined with the periodic boundary condition so that the total energy is conserved. The most appropriate formulation of the Coulomb interaction consistent with the periodic boundary condition is related to the Ewald sum method with a minimum image approximation.[6,13] An electron is assumed to interact with $N-1$ other electrons in the $L\times L$ simulation square through specifically defined distances. The distance of electrons i and j in the minimum image approximation is given by the length of the minimum image vector r_{ij} defined as follows. Let $\mathbf{a}_x=(L,0)$ and $\mathbf{a}_y=(0,L)$. Then the minimum image vec-

tor is given by $r_{ij} = x_j - x_i - n_x a_x - n_y a_y$, where n_x and n_y are chosen to be the integers to minimize the length $|r_{ij}|$.

When electron i or j crosses the axis $x = L$, the integer n_x giving the minimum image vector r_{ij} changes by unity, but the distance itself remains the same, causing no artificial change in the Coulomb energy. Thus, the minimum image approximation satisfies two requirements: do not break the energy conservation law and have an electron interact with the same number of other electrons throughout the simulation. The approximation has an important translational symmetry that the original Ewald sum possesses, which is that the Coulomb potential of an electron does not change under a spatial translation by a_x or a_y and this makes the approximation *completely different* from a usual simple truncation.[6,13]

In molecular dynamics, we update the position x and momentum p with the predictor-corrector method by[13]

$$x(i+1) = x(i) + p(i)\Delta t + f[x(i)](\Delta t)^2/2 , \qquad (1)$$

$$p(i+1) = p(i) + \{f[x(i)] + f[x(i+1)]\}\Delta t/2 , \qquad (2)$$

where $x(i)$ and $p(i)$ indicate the functional values of $x(t)$ and $p(t)$ at the ith time step of period Δt, and f is the force, which is a function of the electron coordinate x (in the units of $m = 1$). This algorithm is second order accurate with respect to Δt and is quite stable since the future force term $f[x(i+1)]$ gives feedback in (2) to determine $p(i+1)$. In fact, the elimination of the momentum terms from (1) and (2) results in Verlet's algorithm,[14] which is known to be second order accurate and also quite stable. With the use of double precision variables in the program to minimize round-off errors, and with the choice of $\Delta t = 10^{-17}$ s to maintain the high accuracy, the summations of electron kinetic energy, 2D potential energy, and interparticle Coulomb energy remains constant to five significant digits for standard runs of $\sim 10^2$ ps in simulations started with an appropriate initial condition (on this time scale, practically no phonon scattering occurs, but it is easy to include the phonon events in the energy conservation determination).

Finding an initial condition is not trivial, because of the Coulomb interaction. If any electrons are unusually close to one another in an initial condition, the interparticle Coulomb energy will lead to a rapid rise in electron kinetic energy and will cause an artificial heating of the electron system. We perform a preliminary simulation, before running a real simulation, to find an appropriate initial condition, using a molecular-dynamics Monte Carlo code with a slight modification. This consists of adding a perturbation to scale the x and y components of the electron momentum by $(\langle E_{kin} \rangle / k_B T)^{1/2}$ at every $\sim 10^2$ time steps so that the average electron kinetic energy $\langle E_{kin} \rangle$ is reset to the thermal energy $k_B T$. This preliminary simulation can start with any conditions but $\langle E_{kin} \rangle$ is usually chosen much larger than $k_B T$. Typically within ~ 10 ps, $\langle E_{kin} \rangle$ is smoothly reduced to $k_B T$ and maintains that value. As $\langle E_{kin} \rangle$ approaches $k_B T$, the scaling perturbation is gradually turned off since the scaling factor approaches unity. At this stage, an appropriate initial condition is obtained. In essence, this is quite

similar to a simulated annealing of the electron system to find a proper initial condition that is allowed by equilibrium statistical mechanics. This momentum scaling is done only to find an initial condition. After finding an appropriate initial condition, a real simulation is performed using the algorithm discussed above, without any momentum scaling perturbation being necessary. With a properly chosen initial condition, found in the above manner, it is found that the real simulation remains stable and gives excellent energy conservation as noted above.

The real simulation gives raw data consisting of each electron position and momentum at every time step. Using these values, we can evaluate the velocity autocorrelation function $\langle v_x(i)v_x(0) \rangle$, the mean-square displacement $\langle \Delta x^2(i) \rangle$, and the radial-distribution function $g(r)$. We create an Einstein plot of the square of the variance in the particle positions and evaluate the diffusion constant D from its temporal gradient by

$$D = \frac{1}{2} \frac{d}{dt} \langle \Delta x^2(t) \rangle , \qquad (3)$$

which can apply to interacting particles, rather than using the Green-Kubo formula to integrate the correlation function.[15]

The validity of the present treatment for the Coulomb interaction is examined by checking the plasma oscillation period in zero 2D potential. This oscillation can be observed in the velocity autocorrelation function in the present case. Since the dispersion relation for the 2D plasma oscillation is $\omega(q) = (e^2 nq/2\epsilon m)^{1/2}$ in the lowest-order calculation,[16] there is no definite frequency in the limit $q \rightarrow 0$.[17] However, others using 2D molecular dynamics, based on the treatment of the Ewald sum with a much larger number of electrons, see a clear oscillation.[17,18] This puzzling situation has been further clarified by several authors,[19] who examined the dispersion characteristics by studying the peaks of the dynamic structure factor $S(q,\omega)$, which was directly calculated with molecular dynamics. These authors noted that the dispersion curve rises with q and becomes almost flat around $q_0 = \sqrt{\pi n}$. The obtained dispersion shows a discrepancy from the curve $\omega(q) = (e^2 nq/2\epsilon m)^{1/2}$, due to higher-order effects that are automatically included in molecular dynamics. The coupling between the single-particle motion and the collective modes is appreciable only near the flat portion of the spectrum, where the density of states is high. The period corresponding to the flat part of the dispersion is empirically given by 5.2 $(4\pi\epsilon m/e^2 q_0^3)^{1/2}$.[17] The present model also has shown an oscillation, with a period 3.5 ps in the velocity autocorrelation function, which is consistent with the above empirical expression. We have also run a simulation reducing the box size L, with the same choice of $\Delta t = 10^{-17}$ s, with the same number of electrons at the same temperature so that the plasma coupling constant $\Gamma = e^2 q_0/(4\pi\epsilon k_B T)$, which is 6.4 for the present model, increases to 36 to make the Coulomb interaction more dominant. The oscillation in the velocity autocorrelation function has a period 0.20–0.22 ps in this case and it is consistent with the above empirical expression. These agreements sug-

gest that the present approach is viable and yields accurate results. We would further remark that since the structure factor can be calculated in this manner, it should be easy to construct the frequency and wave-vector-dependent dielectric function from it, but leave this to further work.

III. RESULTS AND DISCUSSION

The Coulomb interaction changes the thermal equilibrium distribution of the electrons significantly and is not a small perturbation in transport. The electrons in the 2D potential, with $V_0 = 2.5$ meV at 4.2 K, are apparently localized in the potential minima in the absence of the Coulomb interaction, as the mean-square displacement is a bounded function of time.[5] They stay near the bottom of the potential well and none overcome the potential barrier. However, they are in a mobile phase with the Coulomb interaction present, and the mean-square displacement increases linearly with time.[5] With the Coulomb interaction present, interparticle force spreads the electrons in position, raising their energy state (more potential energy), and allows them to overcome the potential barrier more easily. For this reason, the direct comparison of the magnetoconductance with and without the Coulomb interaction does not make sense, and does not characterize the effect of Coulomb interaction. Thus, only the results with the interaction included will be considered.

In studying the magnetoconductance, we need to simulate for a long time since the magnetic field introduces another time scale—the period of cyclotron motion. Because of impurity scattering and the Coulomb interaction, an electron cannot complete one period of the cyclotron motion unless $\omega_c \tau \gg 1$. Thus, the effect of the magnetic field seems important only when the field is strong so that the cyclotron period is shorter than the mean free time determined by scatterings. However, it has been observed in our simulations that the effect of the magnetic field sometimes persists even if this is not the case. The mean-square displacement shows a small amplitude oscillation around the straight line in the Einstein plot. This has to be accommodated by choosing an appropriately long simulation time, or by an appropriate coarse-graining process. The cyclotron motion period for one flux quantum per unit cell is 14 ps, and the impurity-limited mean free time is 4.6 ps. The correlation time for the Coulomb interaction is estimated to be 3.5 ps, which is the interparticle oscillation period observed in the velocity autocorrelation function.[5] Taking into account
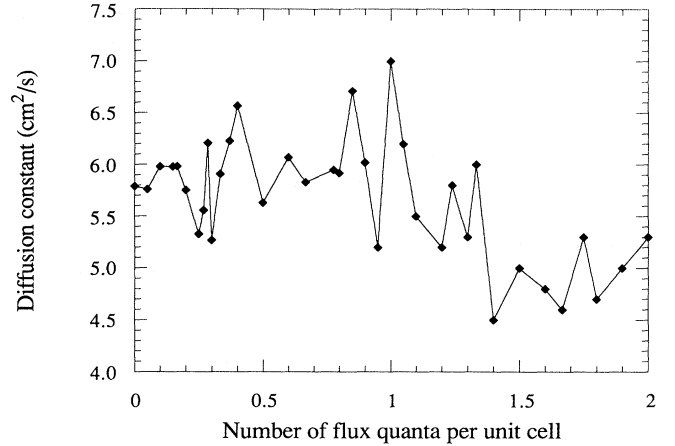

FIG. 1. Conductance as a function of the number of flux quanta per unit cell.

these numbers, we have simulated up to 200 ps to create an Einstein plot for the calculation of the diffusion constant in magnetic fields less than one flux quantum per unit cell, and up to 50 ps for higher fields.

Since the saddle points of the 2D periodic potential are located at $(a/2,0)$, $(0,a/2)$, $(a/2,a)$, and $(a,a/2)$ in the unit cell defined by the two vectors $(a,0)$ and $(0,a)$, the likely diffusion directions for an electron in the middle of the unit cell are $(\pm 1,0)$ and $(0,\pm 1)$. This, along with the small number of particles being used in the simulations, sometimes causes discrepancies in $\langle \Delta x^2 \rangle$ and $\langle \Delta y^2 \rangle$, although these are averaged from the data with long enough simulation times. In order to minimize statistical error, simulations with several different initial configurations of electrons are performed and a further average is taken.

Figure 1 shows the calculated magnetoconductance as a function of the number of flux quanta per unit cell. (For the cell dimensions chosen, one flux quantum per unit cell corresponds to 0.162 T.) The magnetoconductance shows an irregular oscillation which, as a general trend, seems to decrease with the magnetic field. According to the pinball model,[4] resistance maxima (conductance minima) occur when the cyclotron orbit encloses a specific number of antidots with the orbit center fixed in space, called a pinning orbit, while resistance minima (conductance maxima) occur when the cyclotron orbit is not commensurate with the lattice period. In Table I, the

TABLE I. Magnetic fields for pinning orbits.

Antidots	Radius	Calculated B with $\langle E_{kin} \rangle = 0.36$ meV	Calculated B with $\langle E_{kin} \rangle = 0.50$ meV	Observed B
1	$0.50a$	$1.24\Phi_0$	$1.46\Phi_0$	$1.20\Phi_0 - 1.40\Phi_0$
2	$0.81a$	$0.76\Phi_0$	$0.90\Phi_0$	$0.95\Phi_0$
4	$1.14a$	$0.54\Phi_0$	$0.64\Phi_0$	$0.66\Phi_0$
9	$1.71a$	$0.36\Phi_0$	$0.43\Phi_0$	$0.50\Phi_0$
21	$2.53a$	$0.24\Phi_0$	$0.29\Phi_0$	$0.25\Phi_0 - 0.30\Phi_0$

first two columns show the number of antidots and the corresponding pinning orbit radius, respectively, for pinning orbits in the pinball model. The third column shows the calculated magnetic fields for pinning orbits with the assumption that the average electron kinetic energy $\langle E_{kin} \rangle$ is 0.36 meV, and the fourth column also shows the calculated magnetic fields with the assumption that $\langle E_{kin} \rangle$ is 0.50 meV. The observed magnetic fields for the local conductance minima are listed in the fifth column. In the original pinball model,[4] the potential is constant except at the antidot sites and the Fermi energy can be safely used when evaluating the cyclotron radius since the kinetic energy does not change with the spatial position of an electron. On the other hand, with the summation of the cosine functions used here, the kinetic energy changes with the spatial position of an electron and an average value has to be used. One possibility is the thermal energy 0.36 meV and another is the average kinetic energy 0.50 meV when the electrons are near the bottom of the potential well. This will be discussed later.

The second assumption, the average kinetic energy $\langle E_{kin} \rangle = 0.50$ meV, seems better able to explain the observed magnetic fields for the conductance minima. However, two important characteristics in the original pinball model are not observed. First, the pinning orbit $n = 1$ should have the strongest localization effect, giving the smallest conductance. The pinning effect should be weaker with increasing n and the oscillation should fade out in smaller magnetic fields. Second, geometrically, no pinning orbit should be allowed in magnetic fields higher than that of $n = 1$. Thus, the conductance should increase for these higher fields. These two characteristics are not observed in Fig. 1. We also note that the oscillations are not periodic in $1/B$, or in B, which are the expectations from a quantum-mechanical model.[8]

Figure 2 shows the real-space trajectory of a typical

electron during 100 ps, for 0.3 flux quanta per unit cell, which corresponds to a small conductance case. The magnetic-field direction is into the page, so that the cyclotron motion of an electron is clockwise. Because of the impurity scattering and the Coulomb interaction, the real-space trajectory is very complicated. The electron changes its velocity suddenly due to scattering and the cyclotron motion cannot be completed. In the figure, the electron starts at the upper-middle unit cell (where the row of the unit cell is first specified by upper, middle, or lower, and the column of the unit cell is then specified by left, middle, or right, respectively). The electron moves along the direction specified by arrow 1 and leaves the upper-right unit cell, as indicated by arrow 2. Because of the periodic boundary condition, the electron enters the lower-right unit cell, as indicated by arrow 3, and moves along the directions of arrows 4, 5, 6, and 7, forming a clockwise trajectory. During this travel, the electron shows a complicated, singular trajectory due to the Coulomb interaction and the impurity scattering. At 100 ps, the electron finally arrives at the upper-middle unit cell. Since this electron performs a clockwise correlated motion and tends to return to the starting point, this electron gives only a small contribution to the conductance, and can be thought of as being "pinned" in an orbit centered around as many as 21 antidots.

In Fig. 3, the chaotic change of the energy for the same electron is shown. Although the individual kinetic and 2D potential energies change significantly with time as shown in the figure, the total energy of the particles is again conserved. The electron kinetic energy for this particle oscillates in the range 0–2.2 meV with time due to the 2D plasma oscillation. The average total maximum of the kinetic energy is estimated to be 0.5 meV, and this is the motivation to use this value when evaluating the cyclotron radius in Table I. The kinetic energy is almost zero either when the electron is overcoming the potential barrier or when the electron has a maximum displacement in the 2D plasma oscillation. The oscillation in the 2D potential energy is mostly in phase with that in the ki-
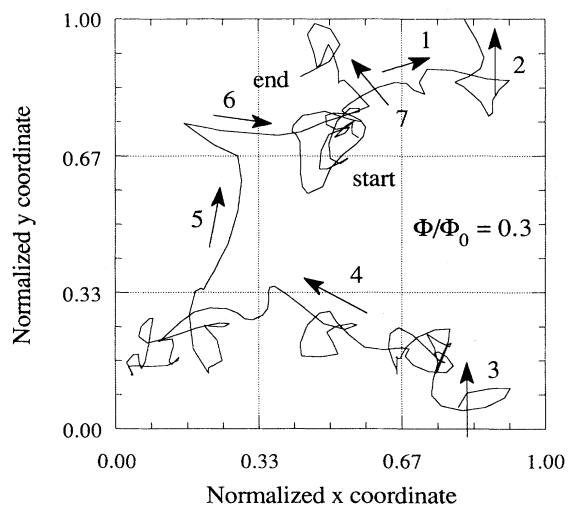

FIG. 2. Real-space trajectory of a typical electron for 0.3 flux quanta per unit cell during 100 ps. The distance is normalized to the side length of the simulation box L and the dotted lines indicate the unit cells.
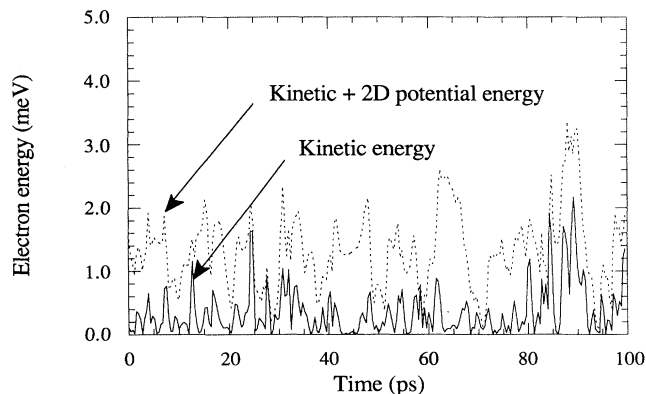

FIG. 3. Time evolution of the energy for the electron of Fig. 2 for 0.3 flux quanta per unit cell during 100 ps. The solid line is the kinetic energy and the dotted line is the summation of the kinetic energy and the 2D potential energy.
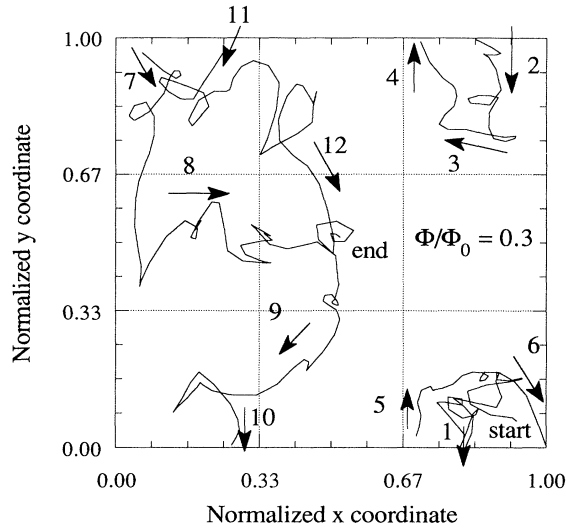
FIG. 4. Real-space trajectory of a second electron for 0.3 flux quanta per unit cell during 100 ps. The distance is normalized to the side length of the simulation box L and the dotted lines indicate the unit cells.

netic energy and this is evidence that the oscillation is mainly due to the 2D plasma oscillation, rather than the classical single-particle oscillation at the bottom of the well. If it were a classical oscillation at the bottom of the well, then the 2D potential energy would be out of phase with the kinetic energy and the summation of the 2D potential energy and the kinetic energy would be constant, which is not the case here.

We can find similar characteristics in the real-space trajectory and the time evolution of energy for a second electron, shown in Figs. 4 and 5, respectively. The electron starts at the lower-right unit cell, moves along arrow 1, and leaves the unit cell. Because of the periodic
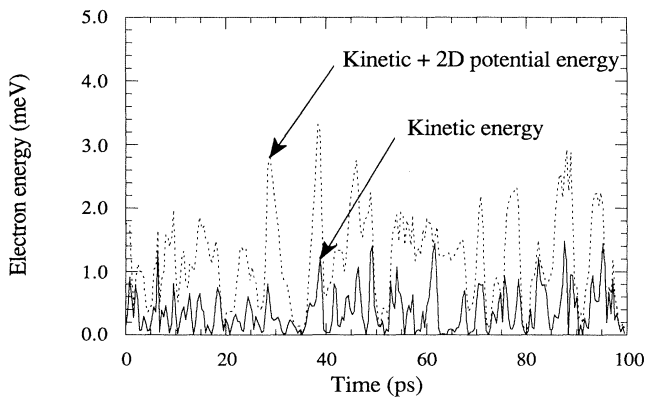
boundary condition, the electron enters the upper-right unit cell and performs a clockwise motion as indicated by arrows 2, 3, and 4. The electron again leaves the upper-right unit cell, reenters the lower-right unit cell, and performs a circular motion along arrows 5 and 6. Then the electron leaves the lower-right unit cell and enters the upper-left unit cell. The electron moves along arrows 7, 8, 9, and 10 and leaves the lower-left unit cell. The electron enters the upper-left unit cell by the periodic boundary condition, and performs a clockwise circular motion as indicated by arrows 11 and 12, finishing the motion in the middle-middle unit cell at 100 ps. This electron drew a closed orbit twice: one is the orbit along arrows 1 through 6 and the other is the orbit along arrows 7 through 11, again resulting in "pinning" behavior. The time evolution of the energy shown in Fig. 5 is essentially the same. The oscillation in the 2D potential energy is in phase with that in the kinetic energy and this indicates that the oscillation is mainly due to the 2D plasma oscillation.

Figure 6 shows the real-space trajectory of a typical electron, during 100 ps, for 0.1 flux quanta per unit cell, which corresponds to a large conductance case, and Fig. 7 is the corresponding time evolution of the energy. The magnetic-field direction is also into the figure so that the cyclotron motion of an electron is clockwise, but the clockwise trajectory is not clear because of the weak incommensurate magnetic field. In Fig. 6, the electron starts in the middle-right unit cell. The electron moves along arrows 1, 2, 3, and 4. It just wanders the potential minima and a systematic clockwise motion is not observed. The electron leaves the middle-right unit cell and enters the middle-left unit cell. Then the electron moves straight as indicated by arrows 6, 7, and 8, and leaves the upper-middle unit cell. The electron enters the lower-

FIG. 5. Time evolution of the energy for the electron of Fig. 4 for 0.3 flux quanta per unit cell during 100 ps. The solid line is the kinetic energy and the dotted line is the summation of the kinetic energy and the 2D potential energy.
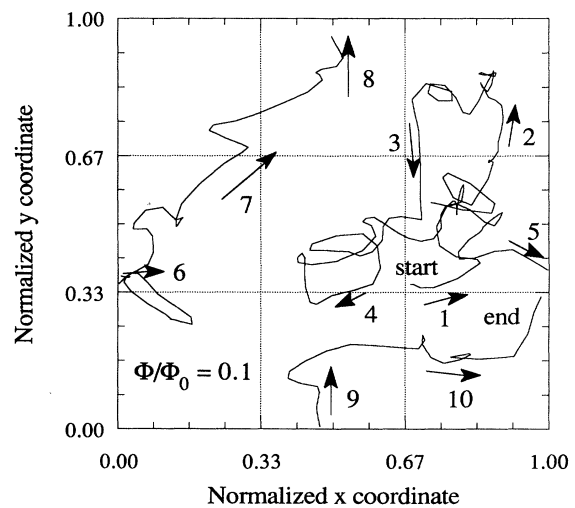

FIG. 6. Real-space trajectory of a typical electron for 0.1 flux quanta per unit cell during 100 ps. The distance is normalized to the side length of the simulation box L and the dotted lines indicate the unit cells.
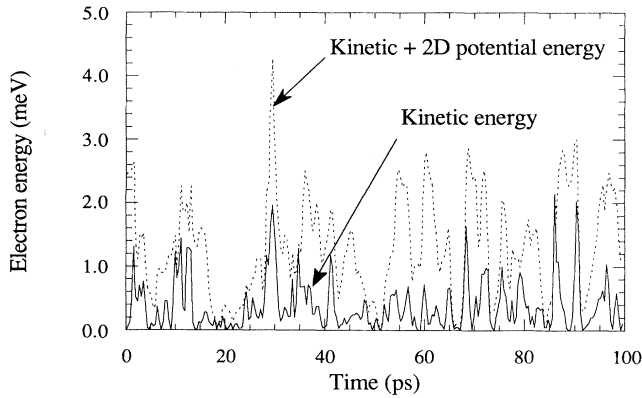
FIG. 7. Time evolution of the energy for the electron of Fig. 6 for 0.1 flux quanta per unit cell during 100 ps. The solid line is the kinetic energy and the dotted line is the summation of the kinetic energy and the 2D potential energy.
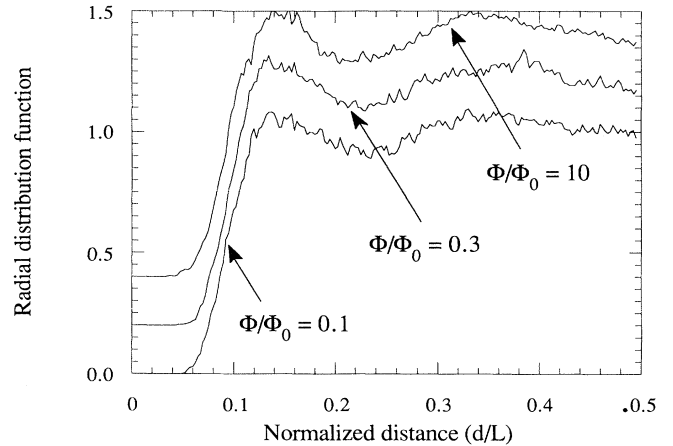

FIG. 8. Radial-distribution function for 0.1, 0.3, and 10 flux quanta per unit cell. For clarity, the functions for 0.3 and 10 flux quanta are shifted by 0.2 and 0.4, respectively.

middle unit cell and moves along arrows 9 and 10. Systematic, correlated circular motion is not observed and therefore the conductance is larger. The time evolution of the energy in Fig. 7 shows the same characteristics as that in Fig. 5. The oscillation in energy can be attributed to the 2D plasma oscillation and the magnetic field does not change the thermodynamical property of the system.

As has been discussed so far, the presence of the Coulomb interaction does not destroy the mechanism of the pinball model. No distinct cyclotron orbit can be completed, but the correlated circular motion is still observed in the small conductance cases, corresponding to pinning orbits, and this is the mechanism of the structure seen in Fig. 1 (and, presumably in the experiments). Because of the Coulomb interaction and impurity scattering, the electrons may change their orbit suddenly. However, this at most causes a short stay in a particular unit cell. The electrons will move to neighboring unit cells and the magnetic field determines which cells are preferred. This indicates that the pinball model has a much wider applicability than expected originally, and can explain the magnetoresistance peaks experimentally observed. The model can be applicable even to the case of lower electron densities where the screening is not strong and the Fermi energy is comparable to the thermal energy.

The change in magnetoconductance is due to the correlated circular motion and *not* due to the real-space rearrangement (or localization) of the electrons for different magnetic fields. In order to see this, the radial-distribution functions for three magnetic fields, 0.1, 0.3, and 10 flux quanta per unit cell, are shown in Fig. 8. For clarity, the functions for 0.3 and 10 flux quanta are offset by 0.2 and 0.4 units, respectively. The case with 10 flux quanta per unit cell is a special trial simulation to see whether spatial order is observed in this range of the magnetic field. The corresponding diffusion constant is significantly different for these three cases, 6.0, 5.3, and 1.9 cm^2/s, respectively. The diffusion constant for 10 flux quanta is quite small and this is because the diffusion con-

stant is expected to behave as $1/[1+(\omega_c\tau)^2]$ in larger magnetic fields, if the 2D periodic potential plays a negligible role. As a general trend, the diffusion constant decreases with increasing magnetic field. As is obvious in Fig. 8, no essential difference can be seen in the radial-distribution functions, in spite of a change in the magnetoconductance, even in the case of 10 flux quanta. Thus, the change in magnetoconductance is not due to a change in spatial order of electrons.

One possible reason why scatterings do not destroy the pinball picture completely is the nature of the Coulomb interaction. The Coulomb interaction conserves the total momentum of the entire electron system. An individual electron may create a singular trajectory, but if we gather several electrons and observe the motion of the center of mass, it will not be significantly different from a cyclotron orbit, although there would be an exchange of electrons among groups whose centers of mass perform a cyclotron motion.

IV. CONCLUSIONS

We have studied the magnetotransport properties of the LSSL, a 2D electron system in a 2D periodic potential, with a Monte Carlo technique, where the effect of the magnetic field and the interparticle Coulomb interaction are included through a Lorentz force, with the latter interaction treated via a molecular-dynamics method within a minimum image approximation. Excellent numerical energy conservation is achieved by adopting a predictor-corrector algorithm to integrate the equations of motion. The simulation shows that the diffusion constant is not a simple decreasing function of the magnetic field, but has a structure with several local minima. This structure is attributed to the correlated circular electron motion, and this is reminiscent of the classical pinning orbits in the pinball machine model for a 2D antidot array, even in the presence of the Coulomb interaction. The radial-distribution function shows no significant

difference for different magnetic fields up to ten flux quanta per unit cell, and the magnetoconductance change is not due to a change in the spatial structure of electrons. The present approach can be applicable even to the case of higher electron densities, where the screening is stronger.

ACKNOWLEDGMENT

APPENDIX: 2D ELECTRONS IN A 2D PERIODIC POTENTIAL UNDER A MAGNETIC FIELD

A system of 2D electrons in a 2D periodic potential, with a perpendicular magnetic field oriented normal to the 2D plane, has an unusual energy band structure in the quantum limit. This quantum-mechanical picture does not have a direct connection to the present semiclassical simulation, but the transition should be considered, since some characteristics may survive in the classical counterpart. In most treatments, only two limits are considered: the Onsager limit ($\hbar\omega_c \ll V_0$) and the Landau limit ($\hbar\omega_c \gg V_0$). The smaller of the two energies is then taken to be a perturbation of the larger energy unit, leading either to miniband formation within the Landau levels in the latter case, or to magnetic breakup of the bands formed in the former case. However, there is a third energy. Typically, the LSSL is thought of as a tight-binding superlattice in which the potential amplitude is related to the interaction potential between neighboring quantum wells. But this is a very limited view.

One should consider the quantum wells separately from the interaction potential. Then it is recognized that there are three energies in the problem: the Landau energy, the quantum-well depth, and the interaction potential between neighboring wells. The first of these is set by the magnetic field, and the second by the amplitude of the periodic potential which creates the quantum wells. The third, however, can be varied through the Fermi energy, and hence through the density. If the density is small, and the potential amplitude high, the electrons will be completely localized within the quantum wells, both quantum mechanically and classically. This is observed for the case of $V_0 = 2.5$ meV, discussed in the text, in the absence of the Coulomb interaction. In this case, localization is complete, *regardless of the strength of the magnetic field*. The magnetic field only serves to split the quantum levels in the largely cylindrical quantum wells.[20,21]

On the other hand, if the density is high, so that the

Fermi energy lies above the saddle-point energies of the 2D potential, the electrons behave as nearly free electrons. In fact, for higher densities and Fermi energy, the presence of the potential is largely completely screened and not at all sensed by the electrons. In the high-density regime, the role of the 2D potential is as a perturbation around the nearly-free-electron dynamics, and the Landau regime is recovered. Note, however, that the 2D potential is a perturbation on the nearly-free-electron dynamics, *regardless of the strength of the magnetic field*.

The interesting regime lies between the two limits discussed above, where the electrons are largely localized in the quantum wells, but transfer (by tunneling, for example) between the wells leads to an interaction potential and 2D superlattice minibands, which are mainly formed by tight binding around the quantum-well energy levels (in a magnetic field). Here, however, the strength of the interaction potential is crucial. If the width of the minibands formed from each quantum level is smaller than the separation between these levels, a simple tight-binding picture holds. However, if the width of the miniband formed in this manner is larger than the spacing of the quantum-well levels, an entire new energy structure formed from the hybridization of the many quantum-well levels will occur. This is now the Onsager limit (for small magnetic fields). Again, note that the hybridization occurs for any value of magnetic field, and the critical energy is the interaction overlap energy and its size relative to the quantum-well energy-level spacings (which are magnetic field dependent). It is interesting to note that much of the differences in experimental observations of Refs. 1–3 treat different regimes discussed above.

Finally, we note that the major effect of the quantization is the change in the density of states. As quantization occurs, states are pulled from the continuum into the quantized levels, forming the quantum-well energy levels or the Landau levels. This modification of the density of states cannot be seen in the semiclassical treatment used in the present work. However, if the minibands, be they in the quantum well or in the Landau levels, are closer than $k_B T$, it is unlikely that the modifications of the density of states can be observed. In the present simulations, the thermal energy is 0.36 meV. At ten flux quanta per unit cell, for the dimensions used in the simulation, the Landau-level separation is about 2.8 meV. The density in the simulation is sufficiently large to put the Fermi energy into the second miniband, but the miniband spacing is only expected to be of the order of 0.3 meV from experiments on structures similar to the parameters assumed here.[22] These numbers suggest that the density-of-states quantization is largely washed out by the thermal effects, and indeed only small effects are observed at the low magnetic field considered here.[1]

[1]J. Ma, R. A. Puechner, W. -P. Liu, A. M. Kriman, G. N. Maracas, and D. K. Ferry, Surf. Sci. **229**, 341 (1990).

[2]D. Weiss, K. v. Klitzing, and K. Ploog, Surf. Sci. **229**, 88 (1990); R. R. Gerhardts, D. Weiss, and U. Wulf, Phys. Rev. B **43**, 5192 (1991).

[3]W. S. Alves, P. H. Beton, M. Henini, L. Eaves, P. C. Main, O.

H. Hughes, G. A. Toombs, S. P. Beaumont, and C. D. W. Wilkinson, J. Phys. Condens. Matter **1**, 8257 (1989).

[4]D. Weiss, M. L. Roukes, A. Menschig, P. Grambow, K. v. Klitzing, and G. Weimann, Phys. Rev. Lett. **66**, 2790 (1991).

[5]T. Yamada and D. K. Ferry (unpublished).

[6]P. Lugli and D. K. Ferry, Appl. Phys. Lett. **46**, 594 (1985);

Phys. Rev. Lett. **56**, 1295 (1986); D. K. Ferry, *Semiconductors* (Macmillan, New York, 1991).

[7]F. F. Fang and W. E. Howard, Phys. Rev. Lett. **16**, 797 (1966); F. Stern, Phys. Rev. B **5**, 4891 (1972).

[8]D. R. Hofstadter, Phys. Rev. B **14**, 2239 (1976); D. J. Thouless, Phys. Rep. **110**, 279 (1984).

[9]See, for example, Phys. Today **43**(2) (1990) (special issue on Nanoscale and Ultrafast Devices); *Granular Nanoelectronics,* edited by D. K. Ferry, J. R. Barker, and C. Jacoboni (Plenum, New York, 1990); *Nanostructure and Mesoscopic Systems,* edited by W. P. Kirk and M. A. Reed (Academic, San Diego, 1991); C. W. J. Beenakker and H. van Houten, in *Solid State Physics,* edited by H. Ehrenreich and D. Turnbull (Academic, San Diego, 1991), Vol. 44.

[10]The tradeoff between thermal energy and the Fermi energy in a quasi-two-dimensional gas has been discussed in connection with screening by F. Stern and W. E. Howard, Phys. Rev. **163**, 816 (1967). These authors point out that the screening is little different from the nondegenerate Debye limit for the conditions considered here, and the Fermi energy must be considerably larger than the thermal energy before a transition to Fermi-Thomas screening is necessary. Here, the Fermi energy is sufficiently small that the thermal spread of the Fermi-Dirac distribution cannot be distinguished from its classical counterpart.

[11]One might assume that since the system is near degeneracy, the exchange potential modifications to the Coulomb interaction should be included within the molecular dynamics. This has been done previously by A. M. Kriman, M. J. Kann, D. K. Ferry, and R. Joshi, Phys. Rev. Lett. **65**, 1619 (1991). The modifications that arise from the exchange interaction are only of importance at very high densities, and play no role for the small densities considered here.

[12]For full self-consistency, the 2D potential would have to be updated according to the change of the electron spatial distribution. Here, however, the potential is assumed to be fixed *a priori* throughout the simulation, which is appropriate for lower electron areal densities. Therefore, the Coulomb energy in the text means the interparticle Coulomb energy.

[13]M. P. Allen and D. J. Tildesley, *Computer Simulation of Liquids* (Clarendon, Oxford, 1987); D. J. Adams and G. S. Dubey, J. Comp. Phys. **72**, 156 (1987).

[14]L. Verlet, Phys. Rev. **159**, 98 (1967); **165**, 201 (1968).

[15]One might naively think that this is the diffusion of a test particle. However, this self-diffusion of the carriers is precisely the diffusion constant related to the mobility by the fluctuation-dissipation theorem [see, e.g., R. Kubo, in *Transport Phenomena,* edited by J. Ehlers, K. Hepp, and H. A. Weidenmüller (Springer-Verlag, Berlin, 1974), pp. 75–125], and is normally used in computing the transport properties by ensemble Monte Carlo techniques at low values of the drift field, as is discussed by C. Jacoboni and L. Reggiani, Rev. Mod. Phys. **65**, 645 (1983).

[16]C. C. Grimes, Surf. Sci. **73**, 379 (1978); T. Ando, A. B. Fowler, and F. Stern, Rev. Mod. Phys. **54**, 437 (1982).

[17]J. P. Hansen, D. Levesque, and J. J. Weis, Phys. Rev. Lett. **43**, 979 (1979).

[18]R. C. Gann, S. Chakravarty, and G. V. Chester, Phys. Rev. B **20**, 326 (1979).

[19]H. Totsuji and H. Kakeya, Phys. Rev. A **22**, 1220 (1980); R. K. Kalia, P. Vashishta, S. W. de Leeuw, and A. Rahman, J. Phys. C **14**, L911 (1981).

[20]C. Cohen-Tannoudji, D. Bernard, and L. Franck, *Quantum Mechanics* (Hermann, Paris, 1977).

[21]U. Rössler, in *Quantum Coherence in Mesoscopic Systems,* edited by B. Kramer (Plenum, New York, 1991), pp. 45–62.

[22]E. Paris, J. Ma, A. M. Kriman, D. K. Ferry, and E. Barbier, J. Phys. Condens. Matter **3**, 6605 (1991).